

Volumetrics of CO₂ Storage in Deep Saline Formations

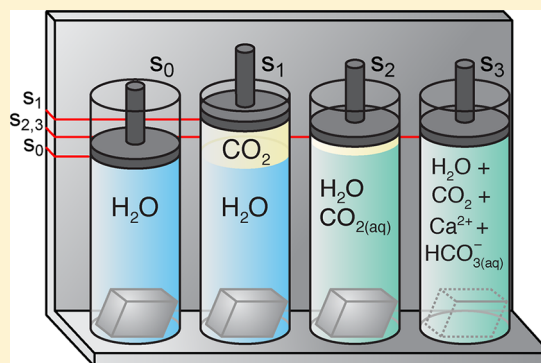
Matthew Steele-MacInnis,^{*,‡} Ryan M. Capobianco,^{‡,‡} Robert Dilmore,[§] Angela Goodman,[§] George Guthrie,[§] J. Donald Rimstidt,^{‡,‡} and Robert J. Bodnar^{‡,‡}

[†]National Energy Technology Laboratory-Regional University Alliance (NETL-RUA), United States

[‡]Department of Geosciences, Virginia Tech, Blacksburg, Virginia 24061, United States

[§]U.S. Department of Energy (DOE), National Energy Technology Laboratory (NETL), P.O. Box 10940, Pittsburgh, Pennsylvania 15236, United States

ABSTRACT: Concern about the role of greenhouse gases in global climate change has generated interest in sequestering CO₂ from fossil-fuel combustion in deep saline formations. Pore space in these formations is initially filled with brine, and space to accommodate injected CO₂ must be generated by displacing brine, and to a lesser extent by compression of brine and rock. The formation volume required to store a given mass of CO₂ depends on the storage mechanism. We compare the equilibrium volumetric requirements of three end-member processes: CO₂ stored as a supercritical fluid (structural or stratigraphic trapping); CO₂ dissolved in pre-existing brine (solubility trapping); and CO₂ solubility enhanced by dissolution of calcite. For typical storage conditions, storing CO₂ by solubility trapping reduces the volume required to store the same amount of CO₂ by structural or stratigraphic trapping by about 50%. Accessibility of CO₂ to brine determines which storage mechanism (structural/stratigraphic versus solubility) dominates at a given time, which is a critical factor in evaluating CO₂ volumetric requirements and long-term storage security.



INTRODUCTION

Managing climate-altering CO₂ emissions by carbon capture and storage (CCS) presents significant economic, political, and technological challenges.^{1–4} One option for mitigating CO₂ emissions is to capture and inject CO₂ into confined saline formations.

Pore space in deep saline formations is initially filled with brine, and no “free” volume is available to accommodate injected CO₂. Injection of CO₂ must, therefore, be accompanied by increase in formation pressure,⁵ compression of fluid and rock, and/or displacement of brine⁵ (Figure 1). Whereas natural subsurface accumulations of CO₂⁶ in environments similar to those proposed for CCS formed slowly and equilibrated with their surroundings over long periods, captured CO₂ will be injected at high volumetric rates over short time spans (tens of years). Numerical modeling has assessed the rate and magnitude of pressure build-up, brine migration, and the potential for CO₂ injection-induced seismicity⁸ associated with rapid injection of large volumes of CO₂ into the subsurface.⁷ Here, we assess equilibrium fluid volume changes in a confined formation after CO₂ injection, based on volumetric properties of the system CO₂-H₂O-NaCl-CaCO₃. The results are relevant to estimates of end-point storage capacity and potential long-term security of CO₂ sequestration in saline formations.

Estimates of reservoir CO₂ storage capacity depend on the storage mechanism(s) being considered.^{2,12} Previous studies estimated CO₂ storage capacity based on structural or

stratigraphic trapping of CO₂, without including the effects of CO₂ or calcite dissolution.^{11,12} However, multiple CO₂ trapping mechanisms define the *ultimate* long-term storage capacity.^{2,13,14} Analyses of fluids from natural CO₂ accumulations indicate that, in at least some cases, the total CO₂ capacity is largely determined by solubility trapping,¹⁵ and thermodynamic modeling has quantified the capacity for CO₂ dissolution into formation waters.^{16,17} Recent studies have emphasized potential benefits of CO₂ injection protocols designed to promote CO₂-brine dissolution, in order to enhance storage security.^{5,18} The effect of CO₂ dissolution and mineral reaction on storage capacity estimates is not yet fully characterized.¹²

The objectives of this study were to compare the subsurface volume required to store an amount of CO₂ as a supercritical fluid with that required to store the same amount of CO₂ as a dissolved component in brine. We applied thermodynamic modeling of the system CO₂-H₂O-NaCl-CaCO₃ to assess the volumetric properties of supercritical CO₂ coexisting with formation brine, CO₂-saturated brine, and CO₂+calcite-saturated brine. Thus, we characterized the volumetric effects

Special Issue: Carbon Sequestration

Received: April 30, 2012

Revised: August 10, 2012

Accepted: August 14, 2012

Published: August 14, 2012

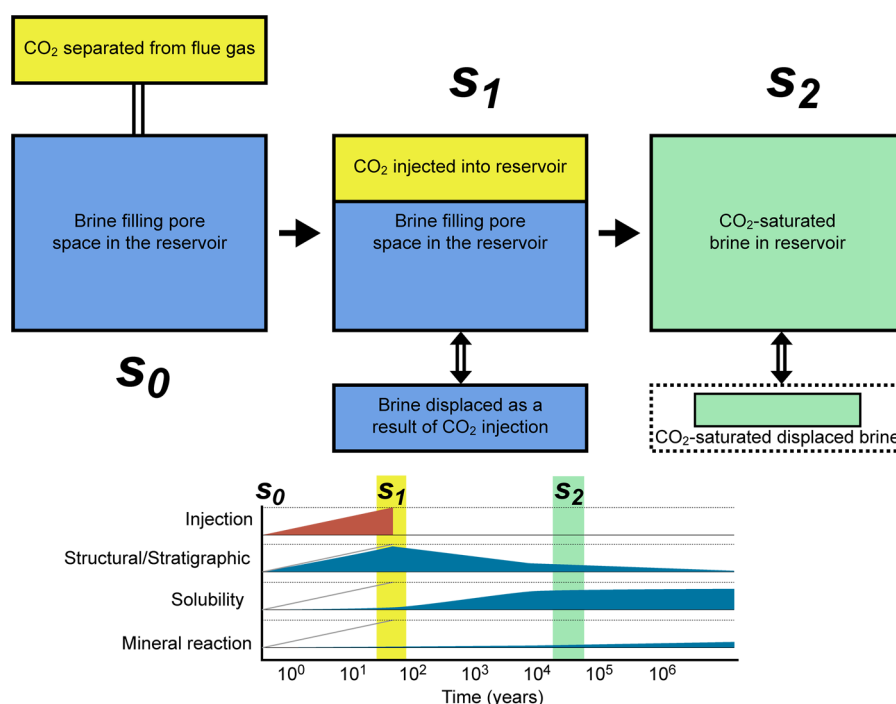


Figure 1. Conceptual model of volume changes associated with various CO₂ storage mechanisms following injection of CO₂ into a saline formation. At s_0 the system is represented by a volume of CO₂ captured from flue gases (yellow box) and a subsurface saline formation in which all of the pore volume is filled with brine (blue box). As a result of injection of supercritical CO₂ into the formation (s_1), an equal volume of brine is displaced from the formation. Some of the CO₂ dissolves into the brine. The volume of the CO₂-saturated brine (green box at s_2) is less than that of the supercritical CO₂ plus brine (s_1) but greater than the original brine volume before CO₂ injection (s_0). Bottom: Approximate time scales over which various trapping mechanisms become significant (modified from the IPCC 2005 report).²

of CO₂ dissolution and reaction with calcite, so that these results can be used to refine storage capacity estimates and to design effective protocols to maximize storage capacity and long-term storage security.

METHODS

Various mechanisms are recognized for geological storage of CO₂, including structural or stratigraphic trapping, trapping as a dissolved component in brine, and trapping by reaction with carbonate minerals.² Our conceptual model for volumetrics of CO₂ storage in saline formations considers the equilibrium end points of these three processes in a stepwise fashion. The total system is represented by an initial mass of CO₂ and a known mass of brine filling the formation pore space (Figure 1). In the first step, the pore space contains only brine. Supercritical CO₂ is injected into the reservoir and a volume of brine equal to the volume of injected CO₂ is displaced from the reservoir (Figure 1; s_1). In this scenario, we do not consider possible changes in reservoir volume owing to compressibility or deformation. In the second step, CO₂ dissolves into the brine to produce a CO₂-saturated solution (Figure 1; s_2). The volume occupied by the CO₂-saturated solution is less than the volume of the injected CO₂ plus brine at step s_1 because the apparent molar volume of dissolved CO₂ is less than the molar volume of supercritical CO₂ at the storage pressure–temperature (PT) conditions.⁹ Thus, fluid volume decreases as the system evolves from s_1 to s_2 , enhancing the storage capacity of the reservoir. In step three, some CO₂ and water react with calcite to form Ca²⁺ and HCO₃[−]. Because of the fast dissolution rates of carbonate minerals compared to silicates, dissolution of calcite will be the most important mineral reaction initially, but additional mineral solution reactions are expected as the system evolves.¹⁰

Fluid volumetric properties were estimated using published equations of state (EOS).^{19–22} The density of supercritical CO₂ is represented by a virial-type EOS.²⁰ The solubility of CO₂ in water and brine is modeled based on Pitzer's formalism.^{21,23} The density of the aqueous fluid is calculated from the apparent molar volumes of CO₂¹⁹ and NaCl²⁴ and the molar volume of H₂O.²² The CO₂ solubility model²¹ has been tested by modeling CO₂ storage in natural brines and yielded good results.²⁵ To compare the volume required to store CO₂ as a supercritical fluid (structural or stratigraphic trapping) with the volume required to store the same amount of CO₂ as a dissolved component in brine (solubility trapping), we selected initial amounts of brine and CO₂ such that all injected CO₂ could be dissolved to produce CO₂-saturated brine. Next, we added increments of calcite and as much additional CO₂ as can be dissolved by reaction with calcite. This approach allows comparison of volumetric changes for three trapping processes – s_1 in which all CO₂ is stored as a supercritical fluid, s_2 in which all CO₂ is stored as a dissolved component in brine, and s_3 in which additional CO₂ is dissolved via the calcite dissolution reaction. All calculations assume constant pressure, although in real-world scenarios, pressure and fluid volume will both increase somewhat upon injection.

Based on various economic and geological constraints, the storage horizon in saline formations will likely be between 1.0 and 4.5 km depth, with temperature of 50–140 °C, and pressure before injection of 10–75 MPa.^{2,14,26} The minimum pressure represents hydrostatic pressure, and the maximum pressure represents 0.6 × lithostatic pressure at the depth of interest. At pressure above this value, vertically oriented hydrofractures may develop.^{27,28} This PT range is highlighted in gray on the PT plots displaying the results. Previous studies

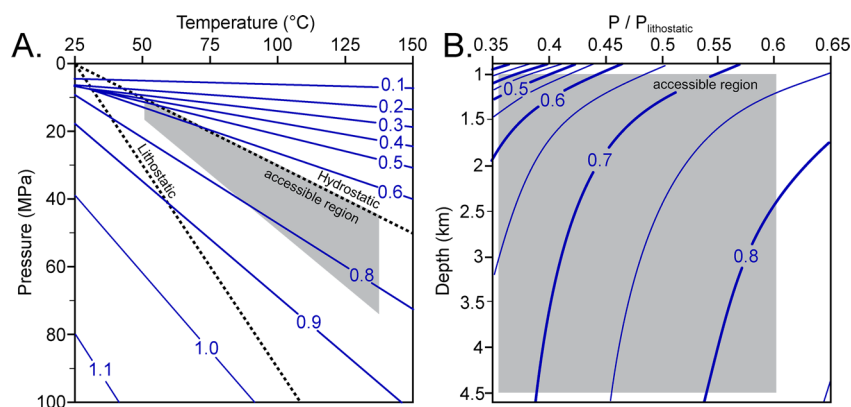


Figure 2. Density of CO₂ (in g/cm³) as a function of pressure and temperature, shown in pressure–temperature space (A) and in depth–fraction of lithostatic pressure space (B). Hydrostatic and lithostatic pressure gradients shown in (A) assume a geothermal gradient of 25 °C/km. The shaded area represents the *PT* conditions technologically and economically accessible for CO₂ storage in saline formations. Notice that A and B contain the same data presented on different axes.

considered the feasibility of injecting large volumes of CO₂ into deep saline formations,^{7,29,30} including various economic and engineering constraints not considered here. Briefly, these studies suggest that pressure build-up during injection may be a limiting factor in determining storage capacity of a formation but that both passive (diffuse leakage) and active (brine extraction) methods can attenuate pressure and allow large-scale injection to proceed.⁷

In the following sections, volumetric changes accompanying *s*₁) CO₂ injection (physical trapping), *s*₂) dissolution in brine, and *s*₃) reaction with calcite are described at discrete times following injection. The motivation for presenting results at discrete stages is to differentiate the volumetric contributions of each mechanism. We emphasize that during and after injection, several trapping mechanisms will likely contribute to the overall storage capacity simultaneously.² However, as a first approximation it is reasonable to separate the various processes based on the different time scales at which each is dominant. Field and laboratory experiments and numerical simulations have semiquantitatively constrained the times required for CO₂ dissolution and mineral reactions in saline aquifers. Although time estimates show wide variability (owing mainly to differences in local reservoir conditions and hydrology), a compilation of those results² suggests overall agreement that physical trapping dominates in the first years to decades, while dissolution of CO₂ and calcite becomes significant over decades to centuries. Other mineral reactions contribute centuries to millennia *after* injection (Figure 1).²

Immediately following CO₂ injection, the system consists of brine and supercritical CO₂, and the system volume equals the initial volume of brine plus the volume of injected supercritical CO₂ (Figure 1, *s*₁). The increase in fluid volume when CO₂ is injected into an H₂O- or H₂O-NaCl-filled formation is

$$\% \text{volume increase} = \frac{\bar{V}_{\text{CO}_2} m_{\text{CO}_2}}{\bar{V}_{\text{H}_2\text{O}-\text{NaCl}} \left(m_{\text{NaCl}} + \frac{1000 \text{ g/kg}}{M_{\text{H}_2\text{O}}} \right)} \times 100\% \quad (1)$$

where \bar{V}_{CO_2} and $\bar{V}_{\text{H}_2\text{O}-\text{NaCl}}$ are the molar volumes of the CO₂ phase and aqueous phase, respectively (cm³/mol), m_{CO_2} and m_{NaCl} are the CO₂ solubility and brine salinity, respectively (mol/kg H₂O), and $M_{\text{H}_2\text{O}}$ is the molar mass of H₂O (g/mol).

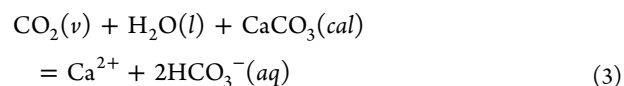
Equation 1 is based on constant mass of H₂O in the system during and after CO₂ injection, representing the pre-existing brine in the pore volume, and the total fluid volume implicitly includes any brine displaced or extracted during injection. Thus, eq 1 (and all subsequent equations) computes volumes in units of cm³ per kg H₂O. Whereas the total amount (number of moles) of fluid in the system is not constant (it increases, as CO₂ is injected), the total mass of H₂O in the system is constant. Therefore, volume changes per kg H₂O represent changes in total fluid volume.

The injected CO₂ phase and aqueous brine are not in chemical equilibrium. Over time CO₂ dissolves into the aqueous phase. The volume change as the system evolves from CO₂-free brine to CO₂-saturated brine is

$$\% \text{volume increase} = \frac{\left(\frac{\bar{V}_{\text{H}_2\text{O}-\text{NaCl}-\text{CO}_2}}{X_{\text{H}_2\text{O}} M_{\text{H}_2\text{O}}} \times 1000 \text{ g/kg} \right)}{\bar{V}_{\text{H}_2\text{O}-\text{NaCl}} \left(m_{\text{NaCl}} + \frac{1000 \text{ g/kg}}{M_{\text{H}_2\text{O}}} \right)} \times 100\% \quad (2)$$

where $\bar{V}_{\text{H}_2\text{O}-\text{NaCl}-\text{CO}_2}$ is the molar volume of the CO₂-saturated aqueous phase (cm³/mol), and $X_{\text{H}_2\text{O}}$ is the mole fraction of H₂O in the aqueous phase.

Reaction with calcite allows dissolution of additional CO₂, according to the reaction



The equilibrium constant for eq 3 was calculated based on the Henry's Law constant for CO₂ dissolution, the calcite solubility product, and the first and second H₂CO₃(aq) dissociation constants. The solubility of calcite (and resulting enhanced CO₂ solubility) was calculated by extrapolating the temperature functions for the relevant equilibrium constants³² over the *PT* range of the model. The volume change of the aqueous phase resulting from calcite dissolution is estimated by approximating the volume occupied by dissolved Ca²⁺ and HCO₃[−] ions based on the apparent molar volume of dissolved CaCl₂.³¹ The volume change is expressed as

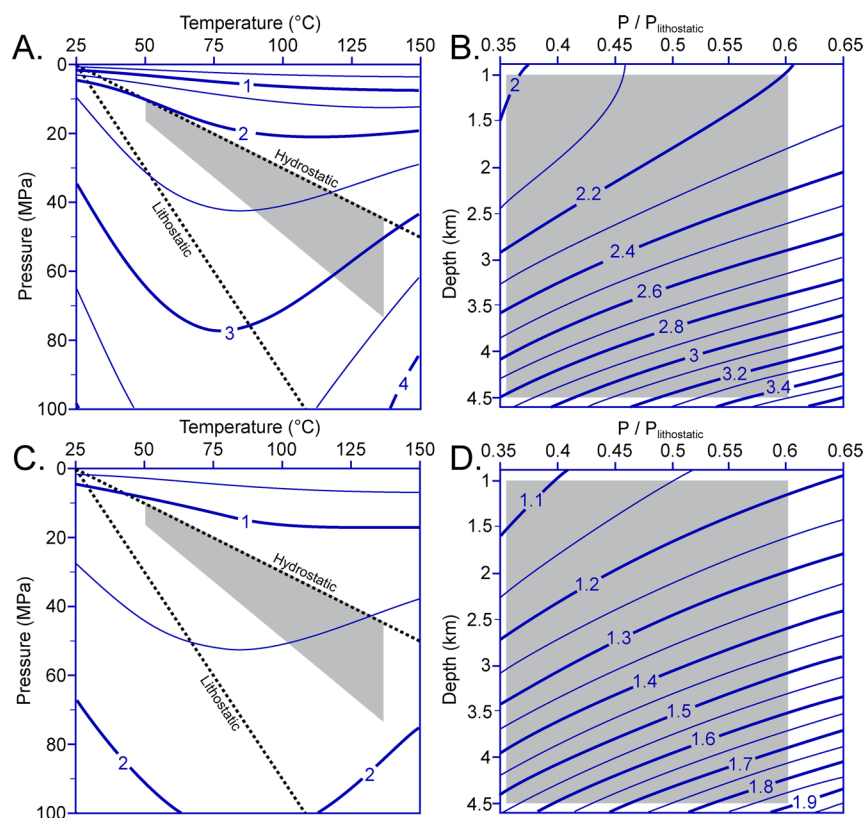


Figure 3. Solubility of CO₂ (mol %) as a function of pressure and temperature in H₂O (A and B) and in 15 wt % NaCl brine (C and D). The data are plotted in pressure–temperature space (A and C) and in depth–fraction of lithostatic pressure space (B and D). The shaded area represents the PT conditions accessible for CO₂ storage in saline formations.

$$\% \text{volume change} = \frac{S_{\text{cal}} V_{\text{Ca}(\text{HCO}_3)_2(\text{aq})}}{V_{\text{CO}_2\text{-saturated solution}} + S_{\text{cal}} V_{\text{Ca}(\text{HCO}_3)_2(\text{aq})}} \times 100\% \quad (4)$$

where $V_{\text{Ca}(\text{HCO}_3)_2(\text{aq})}$ is the apparent molar volume of dissolved calcium and bicarbonate ions, and S_{cal} is the solubility of calcite (mol/kg H₂O).

Our model considers the system H₂O–NaCl–CO₂–CaCO₃, whereas natural saline brines contain other salts, and injected CO₂ may contain other gaseous species. Lack of experimental data over the complete PT range of interest limits our ability to quantitatively model these effects. However, we expect that overall trends in solubility and volumetric properties are reasonably approximated by the H₂O–NaCl–CO₂–CaCO₃ system. For example, CO₂ solubility experiments in natural connate brines from the Oriskany formation (eastern USA) showed good agreement with the CO₂ solubility model used here.^{21,25}

RESULTS AND DISCUSSION

At PT conditions of CO₂ storage in saline formations, CO₂ density ranges from about 0.4 to 0.8 g/cm³ (Figure 2). At the same conditions, the solubility of CO₂ in H₂O ranges from about 2 to 3.4 mol % (Figure 3A and B), and CO₂ solubility in 15 wt % NaCl brine (throughout this section, the term “brine” refers to an aqueous fluid of 15 wt % NaCl) ranges from about 1.1 to 1.8 mol % (Figure 3C and D).^{16,17,21,33}

When an amount of CO₂ equal to the amount required to saturate the aqueous phase (i.e., the amount of CO₂ that could be stored as a dissolved component in the brine) is injected, its

volume is between 75 and 140 cm³ per kg water or 50–70 cm³ per kg brine. During injection, the total fluid volume (*before* dissolution) increases by approximately 7.3 to 10% for pure H₂O (Figure 4A and B) or by about 3.9 to 5.4% for brine (Figure 4C and D). The larger volume increase for H₂O compared to brine reflects higher solubility of CO₂ in pure H₂O compared to brine at the same PT conditions (requiring injection of a greater amount of CO₂ to saturate pure H₂O, Figure 3).

The maximum amount of CO₂ that can be dissolved in brine is limited by the CO₂ solubility at the formation PT conditions (Figure 3). The apparent volume of dissolved CO₂ at saturation is between 40 and 80 cm³ per kg water or 25–55 cm³ per kg brine. Therefore, the volume occupied by the CO₂-saturated aqueous phase is greater than the brine (H₂O) volume before injection (Figure 1). Within the PT range considered here, the volume increases by about 3.5 to 8% if the pore fluid is pure H₂O (Figure 5A) and by about 2.2 to 4% if the pore fluid is brine (Figure 5B).

Owing to the low solubility of calcite, dissolution of calcite increases the volume of the aqueous phase by only 0.01–0.04% (Figure 6). Thus, the contribution of calcite dissolution to the net volume change is insignificant compared to the contributions of supercritical CO₂ or dissolved CO₂.

The volume changes described above (Figures 4–6) are compared to the initial fluid volume before CO₂ injection (Figure 1). We also compared volume change as the CO₂ phase (s_1 ; Figure 1) dissolves into the brine (s_2 ; Figure 1). As shown by the reduced area of the displaced brine box between s_1 and s_2 (Figure 1), dissolution of CO₂ into brine reduces the net fluid volume (compared to the sum of the volumes of brine and CO₂

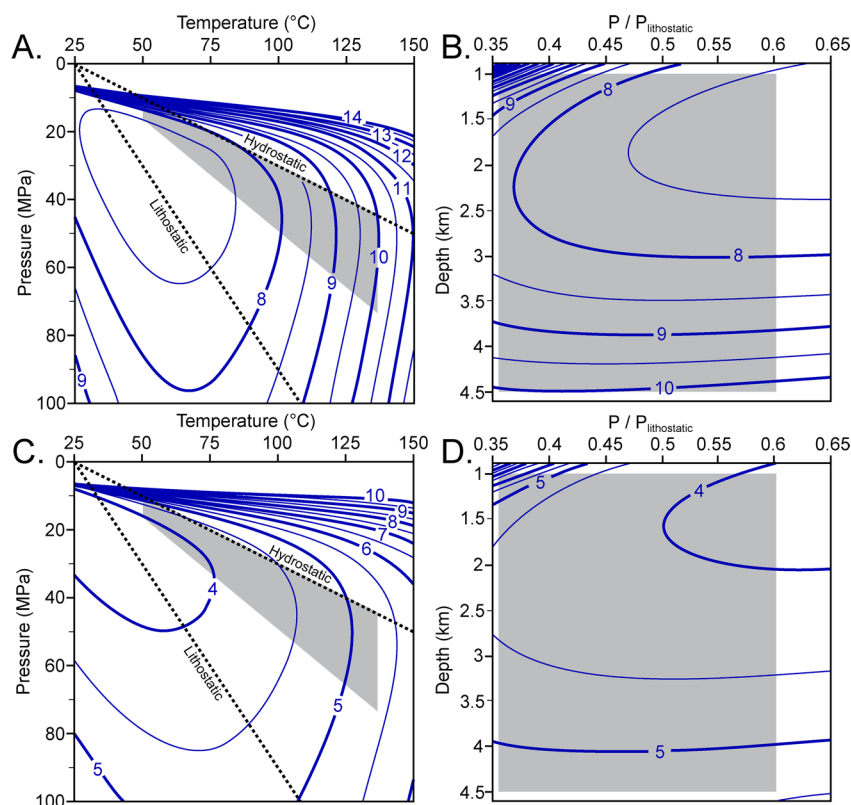


Figure 4. Percent increase in fluid volume when CO₂ is stored in a subsurface reservoir as a separate supercritical fluid. The volume increase represents the percent difference between the volume of the brine *plus* the volume supercritical CO₂ injected (Figure 1, s_1), compared to the volume of brine before injection (Figure 1, s_0). The data are plotted in pressure–temperature space (A and C) and depth–fraction of lithostatic pressure space (B and D). The shaded area represents the PT conditions accessible for CO₂ storage in saline formations. Parts A and B are for H₂O and C and D are for 15 wt % NaCl brine.

immediately following injection). Throughout most of the PT region of CO₂ storage, the apparent volume of dissolved CO₂ is about half of the volume of the same mass of supercritical CO₂. Therefore, the volume decrease from s_1 to s_2 is between 45 and 65%, independent of whether the pore fluid is H₂O (Figure 7A and B) or brine (Figure 7C and D). In other words, although the volume required to store injected CO₂ is greater than the initial brine volume regardless of whether CO₂ is dissolved or is present as a separate supercritical fluid, solubility trapping requires only 50% of the volume required for structural or stratigraphic trapping of the same amount of CO₂.

Previous studies³⁴ have emphasized that dissolution of CO₂ increases the density of the brine, making CO₂-saturated brine negatively buoyant compared to CO₂-free brine. Thus, CO₂-saturated brine will sink in the reservoir,³⁴ enhancing storage security. Based on volumetric modeling, we show that this mechanism has the additional advantage of enhancing storage capacity (Figure 7). The rate of CO₂ dissolution depends on the contact area between the CO₂ and brine phases and how quickly aqueous CO₂ diffuses into the brine. Unassisted, the contribution of solubility trapping becomes significant only after centuries (Figure 1).^{2,9} Some studies have suggested reservoir engineering approaches to accelerate the dissolution of CO₂ into brine, with the aim of enhancing storage security.^{5,18} Our results suggest such procedures will also enhance storage capacity.

As a simple example, consider a target formation at a depth of 2 km, with an injection interval of 50 m. If 28 million tonnes of CO₂ were injected over 30 years, based on simplifying

assumptions for formation properties, injection rate, and fluid characteristics, then the maximum estimated plume radius is 7.4 km.²⁶ A reasonable estimate of microscopic brine displacement efficiency (the proportion of brine that is swept out of the CO₂ plume during injection) for a clastic reservoir is ~50%.¹¹ Therefore, about 50% of the brine initially present in the pore volume within the plume remains available to dissolve CO₂. The residual brine volume accessible for CO₂ dissolution within the plume is 4×10^7 m³. The volume of brine outside the plume but within the cylindrical volume of the maximum plume radius is 8×10^8 m³. The proportion of brine outside the plume that is accessible for CO₂ dissolution is unconstrained, although we can reasonably expect that this proportion will increase with time (as CO₂ diffuses outward from the plume). We consider two endmember scenarios, assuming either 10% or 100% of available brine outside the plume is accessible for CO₂ dissolution.

If CO₂ is injected to a maximum pressure of 90% of the fracture pressure (~54% of lithostatic pressure) and after injection the pressure is allowed to relax back to hydrostatic (~20 MPa in this example), and 10% of the brine outside the plume is accessible for CO₂ dissolution, then about 10% of the injected CO₂ can be dissolved in the available brine (~3% dissolved in residually trapped brine and ~7% dissolved in brine outside the plume). This reduces the total CO₂ volume by ~5%. If 100% of the brine outside of the plume (but within the plume maximum radial extent) were available for CO₂ dissolution, then the proportion of CO₂ that can dissolve increases to about 70%. This results in a reduction in the

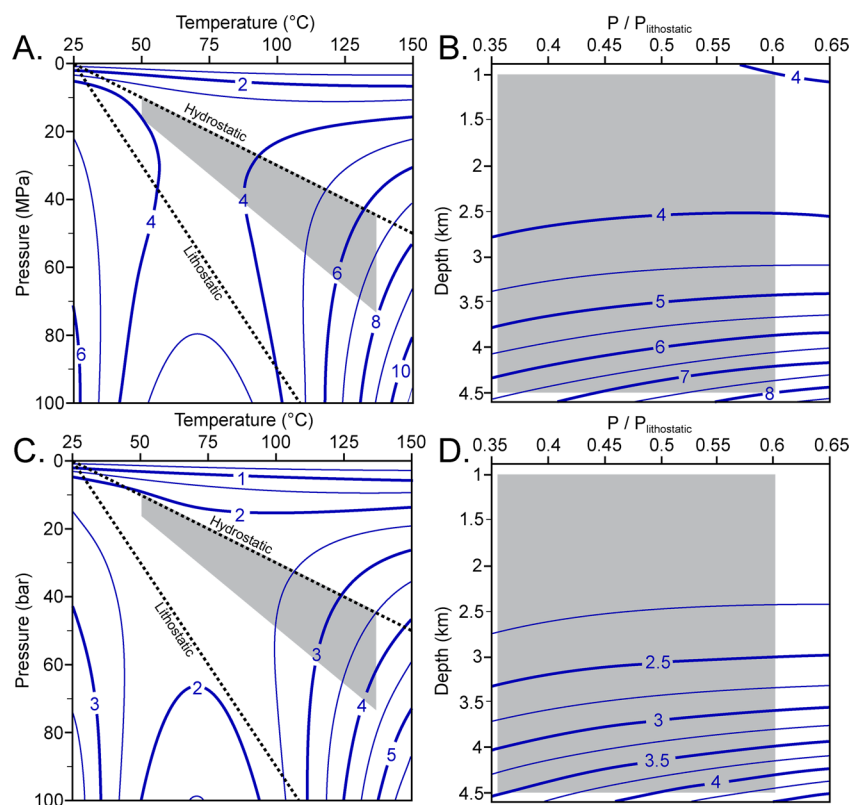


Figure 5. Percent increase in fluid volume after injected CO₂ has dissolved to produce a single-phase, CO₂-saturated brine, shown as percent difference between the volume of CO₂-bearing brine at s_2 compared to the volume of brine before injection (Figure 1, s_0). The data are plotted in pressure–temperature space (A and C) and depth–fraction of lithostatic pressure space (B and D). The shaded area represents the PT conditions accessible for CO₂ storage in saline formations. Parts A and B are for H₂O and C and D are for a 15 wt % NaCl brine.

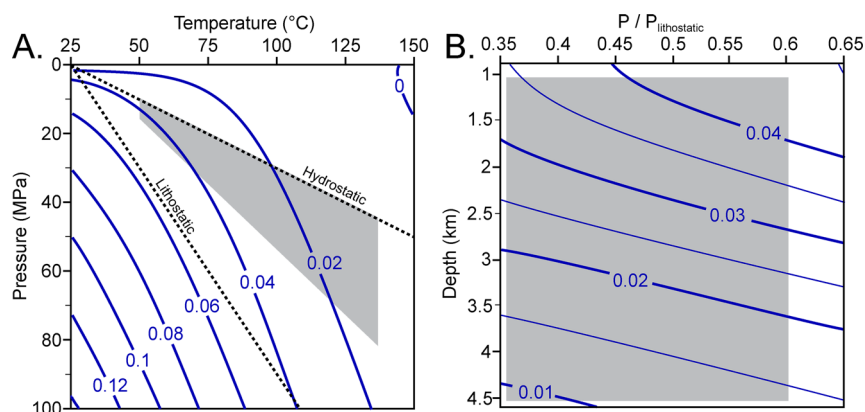


Figure 6. Percent fluid volume change as a result of CO₂-promoted calcite dissolution, relative to the initial volume of pore water. The data are plotted in pressure–temperature space (A) and depth–fraction of lithostatic pressure space (B). The shaded area represents the PT conditions accessible for CO₂ storage in saline formations.

apparent volume of CO₂ of ~45%. Thus, the *accessibility* of brine for CO₂ dissolution is a critical parameter in reducing volumetric requirements associated with solubility trapping. Ultimately, reservoir simulations incorporating lithological and hydrological parameters are required to predict the capacity of solubility trapping in saline formations.¹²

Our results indicate that the CO₂ storage capacity of a formation is influenced by the volumetric changes associated with CO₂ dissolution into brine. We have not attempted comparisons with previous storage capacity estimates from literature because previous comparisons have shown large

variations and sometimes contradictory results, making such comparisons uninformative.¹²

The present study considers final equilibrium states and does not consider effects of fluid flow, pressure gradients, or other factors associated with injection. Figure 1 shows the approximate time intervals over which various trapping mechanisms are expected to become significant, based on reservoir studies and simulations,² but the actual time scales depend on the formation geometry and rock properties.¹² For example, dissolution of CO₂ into brine in a low permeability unit will take significantly longer compared to a high permeability unit.¹² Elucidating the time scales of CO₂-brine-

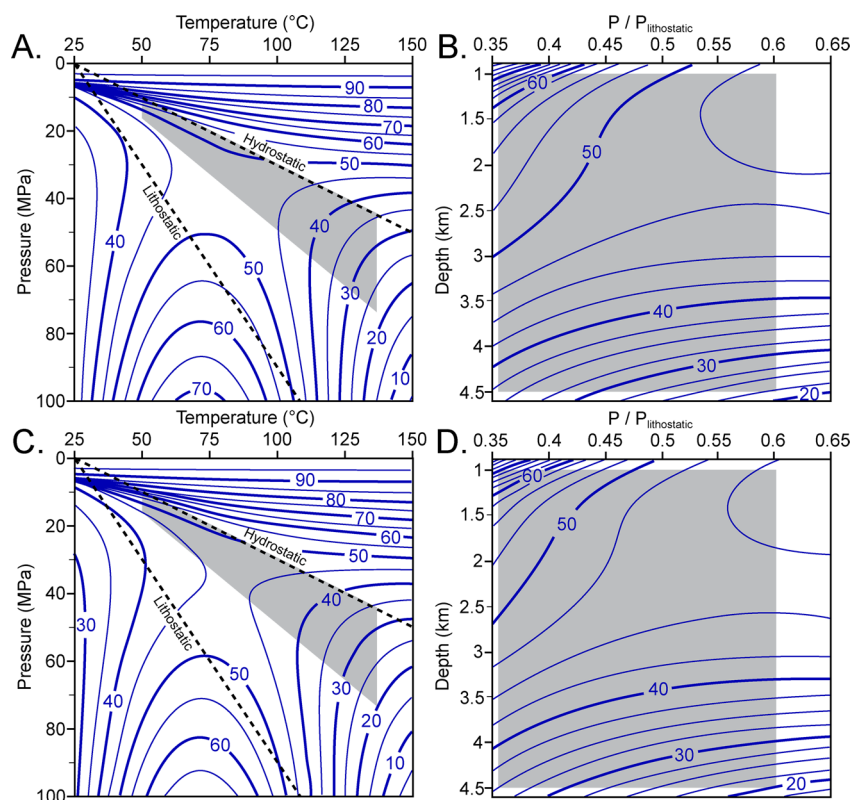


Figure 7. Percent difference in CO_2 apparent volume for CO_2 storage as a supercritical fluid, compared to storage as a dissolved component in brine. The values represent the difference in volume increase between s_2 (Figure 5) and s_1 (Figure 4). The data are plotted in pressure–temperature space (A and C) and depth–fraction of lithostatic pressure space (B and D). The shaded area represents the PT conditions accessible for CO_2 storage in saline formations. Parts A and B are for H_2O and represent the percent difference between values shown in Figure 5A and B for CO_2 storage as a supercritical fluid, compared to volume required for CO_2 storage as a dissolved component in the brine shown in Figure 4A and B). Parts C and D show the same comparison for 15 wt % NaCl brine (Figure 5C and D compared to Figure 4C and D).

mineral interactions during and after injection requires site-specific reservoir simulations on a case-by-case basis.¹² Regardless of the time needed to reach equilibrium, these results document that storing CO_2 as a dissolved component in brine reduces the volume required to store a given amount of CO_2 .

■ IMPLICATIONS

There appear to be significant advantages to solubility trapping for CO_2 storage in brine-filled formations. Our results document that storage volume requirements are reduced by about 50% if CO_2 is dissolved in the brine (solubility trapping), rather than a separate supercritical fluid (structural or stratigraphic trapping). In addition, CO_2 -bearing brine is denser than CO_2 -free brine, so that CO_2 -saturated brine will migrate downward within the formation, thus enhancing long-term storage security. Although the present study does not permit rigorous evaluation of the time scales required to achieve these advantages, the results suggest that storage volume requirements may be reduced by sequestration protocols involving extraction of brine, dissolution of CO_2 into the extracted brine at the surface, followed by reinjection of the CO_2 -saturated brine into the formation.^{5,18} To fully evaluate this alternative operational paradigm for geologic CO_2 storage requires comprehensive reservoir simulations that consider pressure evolution, fluid flow, and temporal changes in CO_2 trapping mechanisms. In addition, associated process

requirements including characterization of life cycle energy, emissions, and economic implications must be considered.

■ AUTHOR INFORMATION

Corresponding Author

*Phone: 1.540.231.8575. Fax: 1.540.231.3386. E-mail: mjmaci@vt.edu.

Notes

Disclaimer: This report was prepared as an account of work sponsored by an agency of the United States Government. Neither the United States Government nor any agency thereof, nor any of their employees, makes any warranty, express or implied, or assumes any legal liability or responsibility for the accuracy, completeness, or usefulness of any information, apparatus, product, or process disclosed, or represents that its use would not infringe privately owned rights. Reference herein to any specific commercial product, process, or service by trade name, trademark, manufacturer, or otherwise does not necessarily constitute or imply its endorsement, recommendation, or favoring by the United States Government or any agency thereof. The views and opinions of authors expressed herein do not necessarily state or reflect those of the United States Government or any agency thereof.

The authors declare no competing financial interest.

■ ACKNOWLEDGMENTS

We thank Alexandra Hakala for valuable discussions and three anonymous reviewers for their insightful and helpful comments

on an earlier version of this manuscript. We also thank David Dzombak and Daniel Giammar for their editorial advice. This research effort was partially performed in support of the National Energy Technology Laboratory under Contract DE-FE-0004000. Steele-MacInnis was funded by the Institute for Critical Technology and Applied Science (ICTAS) at Virginia Tech.

REFERENCES

- (1) Alberts, B. Policy-making needs science. *Science* **2010**, 330 (6009), 1287–1287.
- (2) Intergovernmental Panel on Climate Change, Underground geological storage. In *IPCC Special Report on Carbon Dioxide Capture and Storage*; Metz, B., Davidson, O., de Coninck, H. C., Loos, M., Meyer, L. A., Eds.; Cambridge University Press: New York, 2005; pp 195–276.
- (3) Kerr, R. A.; Kintisch, E. Climatologists feel the heat as science meets politics. *Science* **2010**, 330 (6011), 1623.
- (4) Schiermeier, Q. Putting the carbon back: the hundred billion tonne challenge. *Nature* **2006**, 442 (7103), 620–623.
- (5) Buscheck, T. A.; Sun, Y.; Hao, Y.; Wolery, T.; Bourcier, W.; Thompson, A. F. B.; Jones, E. D.; Friedmann, S. J.; Aines, R. D. Combining brine extraction, desalination, and residual-brine reinjection with CO₂ storage in saline formations: Implications for pressure management, capacity, and risk mitigation. *Energy Procedia* **2011**, 4, 4283–4290.
- (6) Gilfillan, S. M.; Ballentine, C. J.; Holland, G.; Blagburn, D.; Sherwood Lollar, B.; Stevens, S.; Schoell, M.; Cassidy, M. The noble gas geochemistry of natural CO₂ gas reservoirs from the Colorado Plateau and Rocky Mountain provinces, USA. *Geochim. Cosmochim. Acta* **2008**, 72 (4), 1174–1198.
- (7) Zhou, Q.; Birkholzer, J. T. On the scale and magnitude of pressure build-up induced by the large-scale storage of CO₂. *Greenhouse Gases: Sci. Technol.* **2011**, 1, 11–20.
- (8) Cappa, F.; Rutqvist, J. Impact of CO₂ geological sequestration on the nucleation of earthquakes. *Geophys. Res. Lett.* **2011**, 38, L17313.
- (9) Gallagher, J. S.; Crovetto, R.; Levelt Sengers, J. M. H. The thermodynamic behavior of the CO₂-H₂O system from 400 to 1000 K, up to 100 MPa and 30% mole fraction of CO₂. *J. Phys. Chem. Ref. Data* **1993**, 22 (2), 431–513.
- (10) Rimstidt, J. D. Gangue mineral transport and deposition. In *Geochemistry of Hydrothermal Ore Deposits*; Barnes, H. L., Ed.; John Wiley & Sons: New York, 1997; pp 487–515.
- (11) Goodman, A.; Hakala, A.; Bromhal, G.; Deel, D.; Rodosta, T.; Frailey, S.; Small, M.; Allen, D.; Romanov, V.; Fazio, J.; Huerta, N.; McIntyre, D.; Kutchko, B.; Guthrie, G. U.S. DOE methodology for the development of geologic storage potential for carbon dioxide at the national and regional scale. *Int. J. Greenhouse Gas Control* **2011**, 5, 952–965.
- (12) Bradshaw, J.; Bachu, S.; Bonijoly, D.; Burruss, R.; Holloway, S.; Christensen, N. P.; Mathiassen, O. M. CO₂ storage capacity estimation: issues and development of standards. *Int. J. Greenhouse Gas Control* **2007**, 1, 62–68.
- (13) Bachu, S.; Adams, J. J. Sequestration of CO₂ in geological media in response to climate change: capacity of deep saline formations to sequester CO₂ in solution. *Energy Convers. Manage.* **2003**, 44, 3151–3175.
- (14) Benson, S. M.; Cole, D. R. CO₂ sequestration in deep sedimentary formations. *Elements* **2008**, 4 (5), 325–331.
- (15) Gilfillan, S. M. V.; Sherwood Lollar, B.; Holland, G.; Blagburn, D.; Stevens, S.; Schoell, M.; Cassidy, M.; Ding, Z.; Zhou, Z.; Lacrampe-Couloume, G.; Ballentine, C. J. Solubility trapping in formation water as dominant CO₂ sink in natural gas fields. *Nature* **2009**, 458, 614–618.
- (16) Spycher, N.; Pruess, K.; Ennis-King, J. CO₂-H₂O mixtures in the geological sequestration of CO₂. I. Assessment and calculation of the mutual solubilities from 12 to 100°C and up to 600 bar. *Geochim. Cosmochim. Acta* **2003**, 67 (16), 3015–3031.
- (17) Spycher, N.; Pruess, K. CO₂-H₂O mixtures in the geological sequestration of CO₂. II. Partitioning in chloride brines at 12–100°C and up to 600 bar. *Geochim. Cosmochim. Acta* **2005**, 69 (13), 3309–3320.
- (18) Leonenko, Y.; Keith, D. W. Reservoir engineering to accelerate the dissolution of CO₂ stored in formations. *Environ. Sci. Technol.* **2010**, 42, 2742–2747.
- (19) Duan, Z. H.; Hu, J. W.; Li, D. D.; Mao, S. D. Densities of the CO₂-H₂O and CO₂-H₂O-NaCl systems up to 647 K and 100 MPa. *Energy Fuels* **2008**, 22 (3), 1666–1674.
- (20) Duan, Z. H.; Moller, N.; Weare, J. H. An equation of state for the CH₄-CO₂-H₂O system: I. Pure systems from 0 to 1000°C and 0 to 8000 bar. *Geochim. Cosmochim. Acta* **1992**, 56 (7), 2605–2617.
- (21) Duan, Z. H.; Sun, R. An improved model calculating CO₂ solubility in pure water and aqueous NaCl solutions from 273 to 533 K and from 0 to 2000 bar. *Chem. Geol.* **2003**, 193 (3–4), 257–271.
- (22) Hu, J. W.; Duan, Z. H.; Zhu, C.; Chou, I. M. PVTx properties of the CO₂-H₂O and CO₂-H₂O-NaCl systems below 647 K: assessment of experimental data and thermodynamic models. *Chem. Geol.* **2007**, 238 (3–4), 249–267.
- (23) Pitzer, K. S. Thermodynamics of electrolytes: I. Theoretical basis and general equations. *J. Phys. Chem.* **1973**, 77, 268–277.
- (24) Rogers, P. S. Z.; Pitzer, K. S. Volumetric properties of aqueous sodium chloride solutions. *J. Phys. Chem. Ref. Data* **1982**, 11 (1), 15–81.
- (25) Dilmore, R. M.; Allen, D. E.; McCarthy Jones, J. R.; Hedges, S. W.; Soong, Y. Sequestration of dissolved CO₂ in the Oriskany formation. *Environ. Sci. Technol.* **2008**, 42, 2760–2766.
- (26) Nordbotten, J. M.; Celia, M. A.; Bachu, S. Injection and storage of CO₂ in deep saline aquifers: analytical solution for CO₂ plume evolution during injection. *Transp. Porous Media* **2005**, 58, 339–360.
- (27) Hubbert, M. K.; Willis, D. G. Mechanics of hydraulic fracturing. *Trans. A. I. M. E.* **1957**, 210, 153–166.
- (28) Bredehoeft, J. D.; Wolff, R. G.; Keys, W. S.; Shuter, E. Hydraulic fracturing to determine the regional in situ stress field, Piceance Basin, Colorado. *Geol. Soc. Am. Bull.* **1976**, 87, 250–258.
- (29) Ghaderi, S. M.; Keith, D. W.; Leonenko, Y. Feasibility of injecting large volumes of CO₂ into aquifers. *Energy Procedia* **2009**, 1, 3113–3120.
- (30) Ehlig-Economides, C.; Economides, M. J. Sequestering carbon dioxide in a closed underground volume. *J. Pet. Sci. Eng.* **2010**, 70, 123–130.
- (31) Oakes, C. S.; Simonson, J. M.; Bodnar, R. J. Apparent molar volumes of aqueous calcium chloride to 250°C, 400 bar, and from molalities of 0.242 to 6.150. *J. Solution Chem.* **1995**, 24, 897–916.
- (32) Plummer, L. N.; Busenberg, E. The solubilities of calcite, aragonite and vaterite in CO₂-H₂O solutions between 0 and 90 °C, and an evaluation of the aqueous model for the system CaCO₃-CO₂-H₂O. *Geochim. Cosmochim. Acta* **1982**, 46, 1011–1040.
- (33) Takenouchi, S.; Kennedy, G. C. The binary system H₂O-CO₂ at high temperatures and pressures. *Am. J. Sci.* **1964**, 262 (9), 1055–1074.
- (34) Lu, C.; Han, W. S.; Lee, S. Y.; McPherson, B. J.; Lichtner, P. C. Effects of density and mutual solubility of a CO₂-brine system on CO₂ storage in geological formations: “warm” vs. “cold” formations. *Adv. Water Resour.* **2009**, 32 (12), 1685–1702.